Supporting Information

Borjigin et al. 10.1073/pnas.1308285110

SI Materials and Methods

Analysis of Power Spectrum. The original sampling frequency of 1,000 Hz was down-sampled to 500 Hz to reduce computation time. A notch filter was used to remove the 60-Hz artifact and its possible superharmonics. In Fig. 2, the spectrograms using short-time Fourier transform were calculated based on discrete Fourier transform with 2-s segment size and 1 s overlapping for each frequency bin (0.5–250 Hz with 0.5 Hz bin size; spectrogram.m in MatLab Signal Processing Toolbox; MathWorks Inc.). Each segment is windowed with a Hamming window. The absolute power was expressed in log scale (Fig. 2*A*, *Top* and *Middle*). The relative power (Fig. 2*B*) was calculated at each EEG epoch by dividing the absolute power of each frequency bin with the total power over all frequency bands (0.5–250 Hz). Thus, for each EEG epoch, the sum of relative power over all frequency bands should be 100%. The mean and SD of absolute and relative powers was calculated (Fig. 2*B*, *Bottom*) for eight frequency bands: delta (0–5 Hz), theta (5–10 Hz), alpha (10–15 Hz), beta (15–25 Hz), low gamma (γ1; 25–55 Hz), medium gamma (γ2; 80–115 Hz), high gamma (or γ3; 125–145 Hz), and ultra gamma (γ4; 165–250 Hz). The grouping of the gamma bands into the four frequency ranges was designed to avoid the possible artifact contaminations from 60 Hz and its superharmonic. For the mean spectral power, the 10-min-long EEG epochs in the middle of the whole EEG data for waking and anesthesia states, and ∼20-s-long epochs corresponding to CAS3 state were taken from all rats ($n = 9$). To test the statistical significance of the change of spectral powers across three states, repeated-measures one-way ANOVA and Bonferroni's multicomparison were carried out for the eight frequency bands. The adjusted P values by Bonferroni correction are denoted in Fig. 2 ($^*P < 0.05$, $^{**}P < 0.01$, $^{***}P < 0.001$).

Analysis of Coherence. The coherence between EEG channels was measured by amplitude squared coherence $C_{xy}(f)$ (mscohere.m in MATLAB signal toolbox; MathWorks, Inc.), which is a coherence estimate of the input signals x and y using Welch's averaged, modified periodogram method. The magnitude squared coherence estimate $C_{xy}(f)$ is a function of frequency with values between 0 and 1 that indicates how well x corresponds to y at each frequency.

$$C_{xy}(f) = \frac{|P_{xy}(f)|^2}{P_{xx}(f)P_{yy}(f)}, 0 \le C_{xy}(f) \le 1, \quad [1]$$

where $P_{xx}(f)$ and $P_{yy}(f)$ are the power spectral density of x and y and $P_{xy}(f)$ is the cross-power spectrum spectral density. For each rat, the mean coherence among the 15 pairs of six EEG channels was calculated (Fig. 3*A*). Specifically, EEG signal was segmented into 2-s epochs with 1 s overlapping over the whole EEG recording. The magnitude squared coherence estimate was calculated at each epoch and frequency bin (over the frequency range of 0.5–250 Hz) for each rat. The mean and SD of coherence for six EEG channels were then computed for all rats across the three states (waking, anesthesia, and CAS3; Fig. 3*B*). Again, 10-min-long EEG epochs during waking and anesthesia states and 20-s-long EEG epochs in CAS3 states were taken from nine rats. To test the statistical significance of the change in coherence across the three states, repeated-measures one-way ANOVA and Bonferroni's multicomparison tests were carried out for eight frequency bands. The adjusted P values by Bonferroni correction were denoted in Fig. 3*B* ($^*P < 0.05$, $^{***}P < 0.001$).

Analysis of Directional Connectivity. The directional connectivity between EEG channels was measured by normalized symbolic transfer entropy (NSTE), which is a nonlinear and model-free estimation of directional functional connection based on information theory. STE measures the amount of information provided by the additional knowledge from the past of the source signal $X(X^P)$ in the model describing the information between the past $Y(Y^P)$ and the future $Y(Y^F)$ of the target signal Y, which is defined as follows:

$$STE_{X\to Y} = I\left(Y^F; X^P | Y^P\right) = H\left(Y^F | Y^P\right) - H\left(Y^F | X^P, Y^P\right), \quad [2]$$

where $H(Y^F|Y^P)$ is the entropy of the process Y^F, conditional on its past. Each vector for Y^F, X^P, and Y^P is a symbolized vector point. For the appropriate embedding parameters of symbolized vector, three embedding parameters—embedding dimension (d_E), time delay (τ), and prediction time (δ)—are needed. Here we selected the parameter set that provides the maximum information transfer from the source signal to the target signal as the primary connectivity for a given EEG dataset. By investigating the NSTE in the broad parameter space of d_E (from 2 to 10) and τ (from 1 to 30), we fixed the embedding dimension (d_E) at 3, which is the smallest dimension providing a similar NSTE, and found the time delay (τ) producing maximum NSTE. In this parameter space, a vector point could cover from 11.7 ms (with $\tau = 1$ and $d_E = 3$) to 351 ms maximally (with $\tau = 30$ and $d_E = 3$). By taking the maximum NSTE as the primary connectivity for a given EEG dataset, all other processes are nonparametric without subjective decisions for embedding parameters. The prediction time was determined with the time lag (from 1 to 100, 3.9–390 ms), resulting in maximum cross-correlation, assuming the time lag as the interaction delay between the source and target signals.

The potential bias of STE for a given EEG dataset was removed with a shuffled data, and the unbiased STE is normalized as follows:

$$NSTE_{X\to Y} = \frac{STE_{X\to Y} - STE_{X\to Y}^{Shuffled}}{H(Y^F|Y^P)} \in [0, 1], \quad [3]$$

where $STE_{X\to Y}^{Shuffled} = H(Y^F|Y^P) - H(Y^F|X_{Shuff}^P, Y^P)$. X_{Shuff}^P is a shuffled data by replacing the first half to the other half of data. $STE_{X\to Y}^{Shuffled}$ estimates a bias generated by characteristic of given EEG data, not by true causality. Therefore, NSTE is normalized STE (dimensionless), in which the bias of STE is subtracted from the original STE and then divided by the entropy within the target signal, $H(Y^F|Y^P)$. In EEG connectivity, NSTE represents the fraction of information in the target EEG channel not explained by its own past and explained by the source EEG channel. The feedback and feedforward connectivity between frontal and parietal–occipital EEG channels was defined by averaged NSTE. The feedback connectivity ($\overline{NSTE}_{FB}$) was calculated over the eight pairs of EEG channels between the frontal (f)channels and the parietal (p) and occipital (o) channels, which is defined as follows:

$$\overline{NSTE}_{FB} = \frac{1}{n_f \cdot n_p} \sum_{(i,j)=1}^{n_f \cdot n_{p,o}} NSTE_{i\to j}, \quad [4]$$

where $n_f = 2$ and $n_{po} = 4$. The feedforward connectivity ($\overline{NSTE}_{FB}$) from the parietal and occipital channels to the frontal channels

is vice versa. For the application, we first filtered EEG into six frequency bands and segmented the whole-filtered EEG data into 10-s-long EEG epochs without overlapping. Then, $\overline{NSTE}_{FB}$ and $\overline{NSTE}_{FF}$ were sequentially calculated at each epoch. The mean values for waking and anesthesia were calculated with the feedback and feedforward connectivity for 10-min-long EEG epochs over nine rats, but the mean values for CAS3 were calculated with the maximum feedback and feedforward connectivity in CAS3. The short CAS3 epoch of 20 s, which permits selection of only one or two connectivity values, necessitates the choice of the maximum connectivity values to represent the CAS3 state. To test the statistical significance of feedback and feedforward connectivity changes across states, repeated-measures one-way ANOVA and Bonferroni's multicomparison tests were carried out. Adjusted *P* values by Bonferroni correction are denoted in Fig. 4*B* ($^{***}P < 0.001$).

Analysis of Cross-Frequency Coupling. Modulation index (MI) was used for measuring the cross-frequency coupling between gamma and theta rhythms. To measure MI for a given EEG data, EEG signals were first filtered via convolution with a complex Morlet wavelet with width of seven (central frequencies: 2–28 Hz for phases and 2–248 Hz for amplitude envelopes with 2-Hz bin). For each filtered signal, the instantaneous phases $\varnothing_{LF}(t)$ of a lower-frequency band taken by applying Hilbert transform and the amplitude envelope $A(t)_{HF}$ of a higher-frequency band of EEG signal were combined into one composite, complex-valued signal $Z(t) = A(t)_{HF}.e^{-i\varnothing_{LF}(t)}$. If the probability density function of $Z(t) =$ real$[Z(t)]$ + imag$[Z(t)]$ in the complex plan is not radially symmetric, it means that $A(t)_{HF}$ and $\varnothing_{LF}(t)$ share mutual information, or that the distribution of $\varnothing_{LF}(t)$ is nonuniform. MI is defined as the absolute value of the average of $Z(t)$ and measures the degree of asymmetry of the probability density function. MI is used as a metric of coupling between two frequency bands (phases of a lower-frequency band and amplitudes of a higher-frequency band). To test the significance of the asymmetry, 50 surrogate data were generated by shuffling the high-frequency amplitude envelope $A(t)_{HF}$ after dividing it into 1-s sections. This surrogate data retains the mean, variance, and power spectrum of the original signal while removing the temporal ordering between amplitudes. MI was calculated with the population of 50 shuffled amplitude envelopes and phases of a low-frequency signal, generating 50 MI values. A MI value was deemed significant if it reached the top 5% of this distribution of surrogate data. The MatLab toolbox for MI and significance test (1) was used for the computations (www.cs.bris.ac.uk/Research/MachineLearning/pac/). Similar to the power (Fig. 2), coherence (Fig. 3), and connectivity (Fig. 4) analyses, the 10-min-long EEG was taken from waking and anesthetized states, and segmented into 10-s-long EEG epochs. For each epoch, MI of original data and 50 MI of shuffled data were calculated over all pairs of frequency bands (phases: 0.5–30 Hz, amplitudes: 0.5–250 Hz). If MI values of certain frequencies were significant, we used the MI values for the average, otherwise, padded with zero. A total of 3,240 epochs from a 10-min-long EEG data (60 epochs, six EEG channels, and nine rats) were used to create the averaged MI for waking and anesthesia states (Fig. 5). The averaged MI for CAS3 state, in contrast, consisted of 54 epochs (one epoch, six EEG channels, and nine rats), due to its short duration. The 12 different types of phase-amplitude coupling were investigated between the three slow-frequency bands [delta (0.5–5 Hz), theta (5–10 Hz), and alpha (10–15 Hz)] and four fast-frequency bands [low gamma (25–55 Hz), medium gamma (65–115 Hz), high gamma (125–145 Hz), and ultra gamma (145–250 Hz)]. To test the statistical significance of specific coupling compared with the other types of couplings, we applied Friedman test and Dunn's multicomparison test. The adjusted *P* values were calculated by family-wise correction (Fig. 5*B*).

Statistical Analyses. All statistical analyses were carried out in consultation with the Center for Statistical Consultation and Research at the University of Michigan. The statistical analyses were performed using the software GraphPad Prism (version 5.01; GraphPad Software Inc.).

1. Onslow ACE, Bogacz R, Jones MW (2011) Quantifying phase-amplitude coupling in neuronal network oscillations. *Prog Biophys Mol Biol* 105(1-2):49–57.

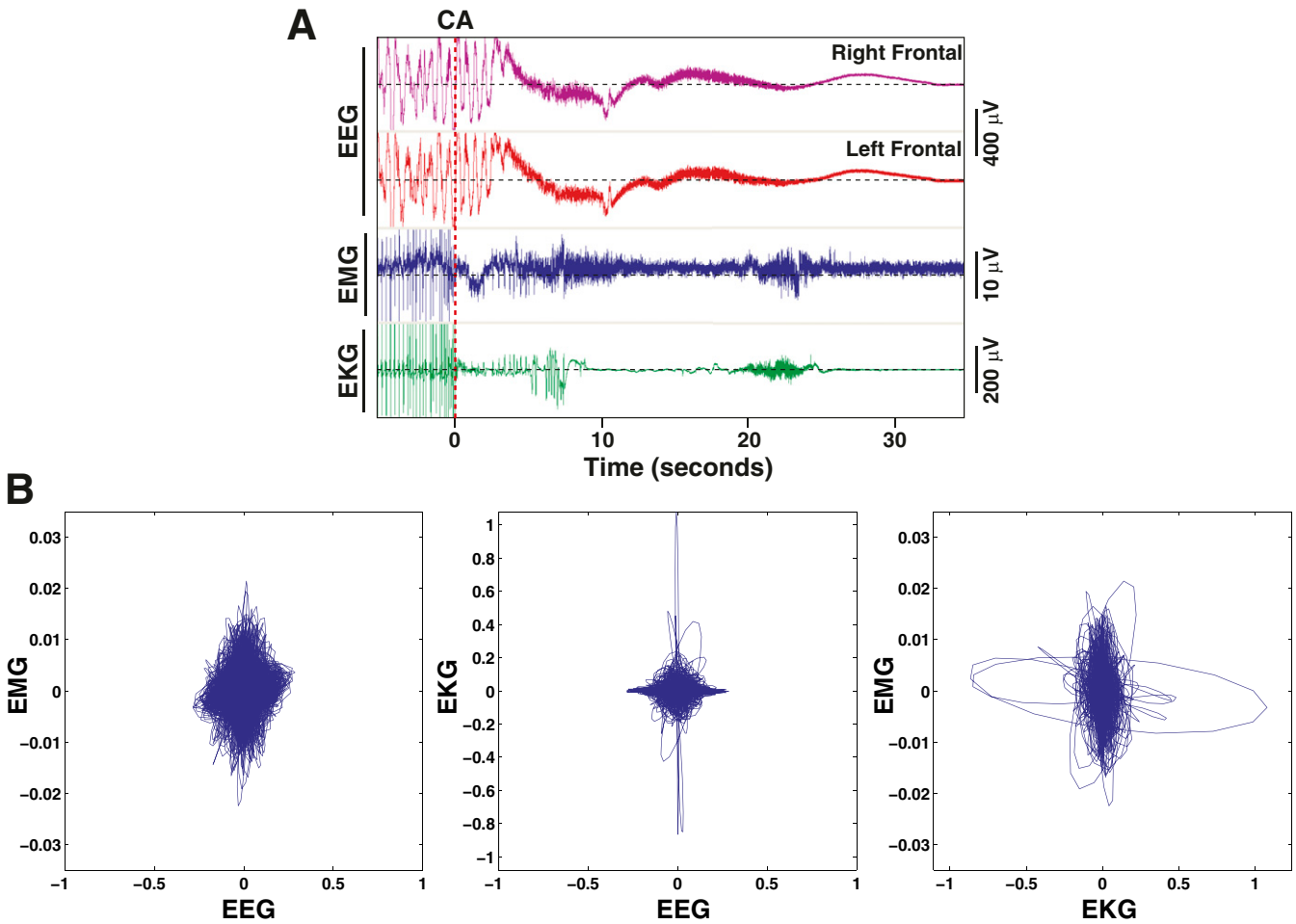

Fig. S1. The scatter plots and Spearman correlation coefficients among EEG, EKG, and EMG signals. (*A*) The unprocessed EEG (right and left frontal areas), EMG, and EKG signals taken from the first 30 s of cardiac arrest in one rat (ID5510). No correlation was visually detected between EEG and EMG, and between EEG and EKG signals. (*B*) The scatter plots for the pairs of signals (EEG, EMG, and EKG) in low-gamma (25–55 Hz) bands for a sample data (ID5510) after cardiac arrest. No significant correlation of EEG with EMG or EKG was found for any of eight frequency bands for three rats (note that EKG signals for three of the nine rats were recorded simultaneously with the EEG signals). Average correlation coefficient for eight frequency bands of the three rats was 0.06 ± 0.042 for left frontal (LF)-EEG and EMG, 0.055 ± 0.029 for LF-EEG and EKG, 0.061 ± 0.044 for right frontal (RF)-EEG, and EMG, 0.054 ± 0.027 for RF-EEG and EKG. These correlation coefficients were all highly significant ($P < 0.01$). Average correlation coefficient between EKG and EMG signals, however, showed strong correlations (0.624 ± 0.26, $P < 0.01$), especially at the lower-frequency bands (<55 Hz).

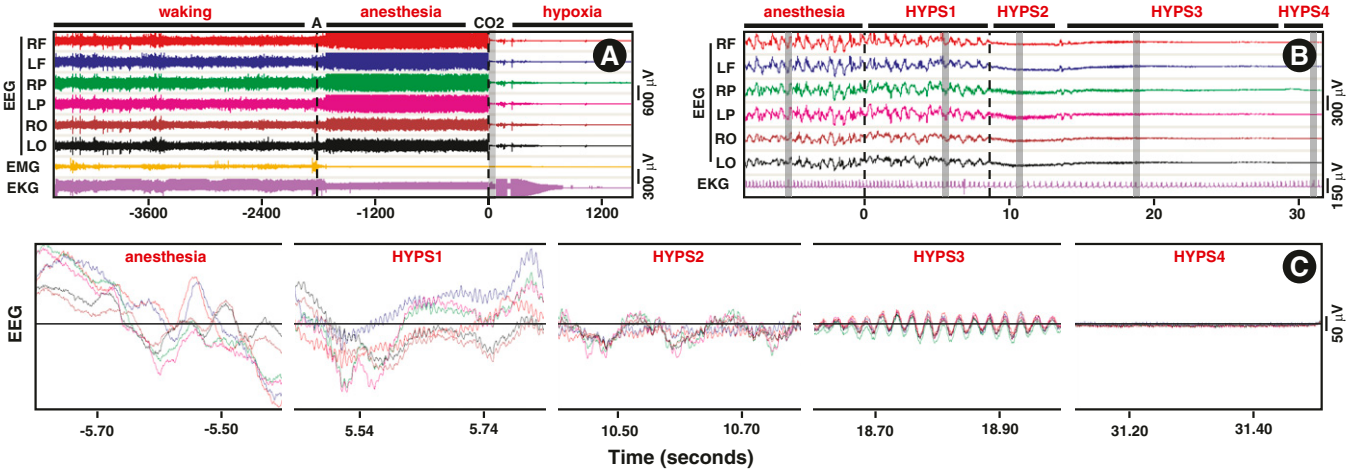

Fig. S2. Global hypoxia activates a well-organized series of high-frequency activity in the dying brain. (*A*) EEG, EMG, and EKG during baseline waking state, anesthesia, and following inhalation of 100% CO_2. EEG was recorded from six regions of the rat brain: the right frontal (RF) and left frontal (LR); right parietal (RP) and left parietal (LP); and right occipital (RO) and left occipital (LO) areas. Anesthesia (A) was induced by intramuscular injection of ketamine and xylazine (black dashed line). Global hypoxia was induced by inhalation of 100% CO_2 for 2 min beginning at time (T) = 0 s. The heart continued to beat for more than 600 s. (*B*) The 40-s segment, shown as a vertical gray bar in *A,* including 8 s before and 32 s after cardiac arrest, was expanded to reveal detailed features. Following CO_2 inhalation, EEG signals maintained regular patterns for a few seconds before transitioning to a period of low-amplitude and high-frequency oscillations for up to 30 s. The period following CO_2 inhalation was divided into four distinct states: hypoxia state 1 (HYPS1) beginning at the T = 0 s and ending at the loss of oxygenated blood pulse (LOP; marked in vertical dashed line at T = 8 s); HYPS2 beginning at LOP and ending at a delta blip (a short burst of delta oscillation) at T = 14 s; HYPS3 beginning at the end of the delta blip and ending when the EEG signal reached below 10 μV at T = 28 s; HYPS4 spanning the remaining hypoxia period after EEG signals were consistently below 10 μV. (*C*) The selected segments in *B* (indicated in vertical gray bars from left to right) were further expanded, and the EEG signals from all six channels were overlaid on top of each other to reveal further details. Unlike the anesthetized state (*Left*), HYPS1 exhibited elevated gamma oscillations near 130 Hz in all six EEG channels. The HYPS2 period exhibited theta oscillations mixed with high-frequency gamma oscillations across all channels. HYPS3, in contrast, was dominated by EEG signals in the low-gamma frequency range (35–50 Hz) that were highly synchronous across all EEG channels. HYPS4 was composed of mostly 300-Hz signals that persisted for as long as recording was continued. Thus, an organized series of neurophysiologic events can be observed at near-death irrespective of the mode of induction—global hypoxia or global ischemia (Fig. 1).

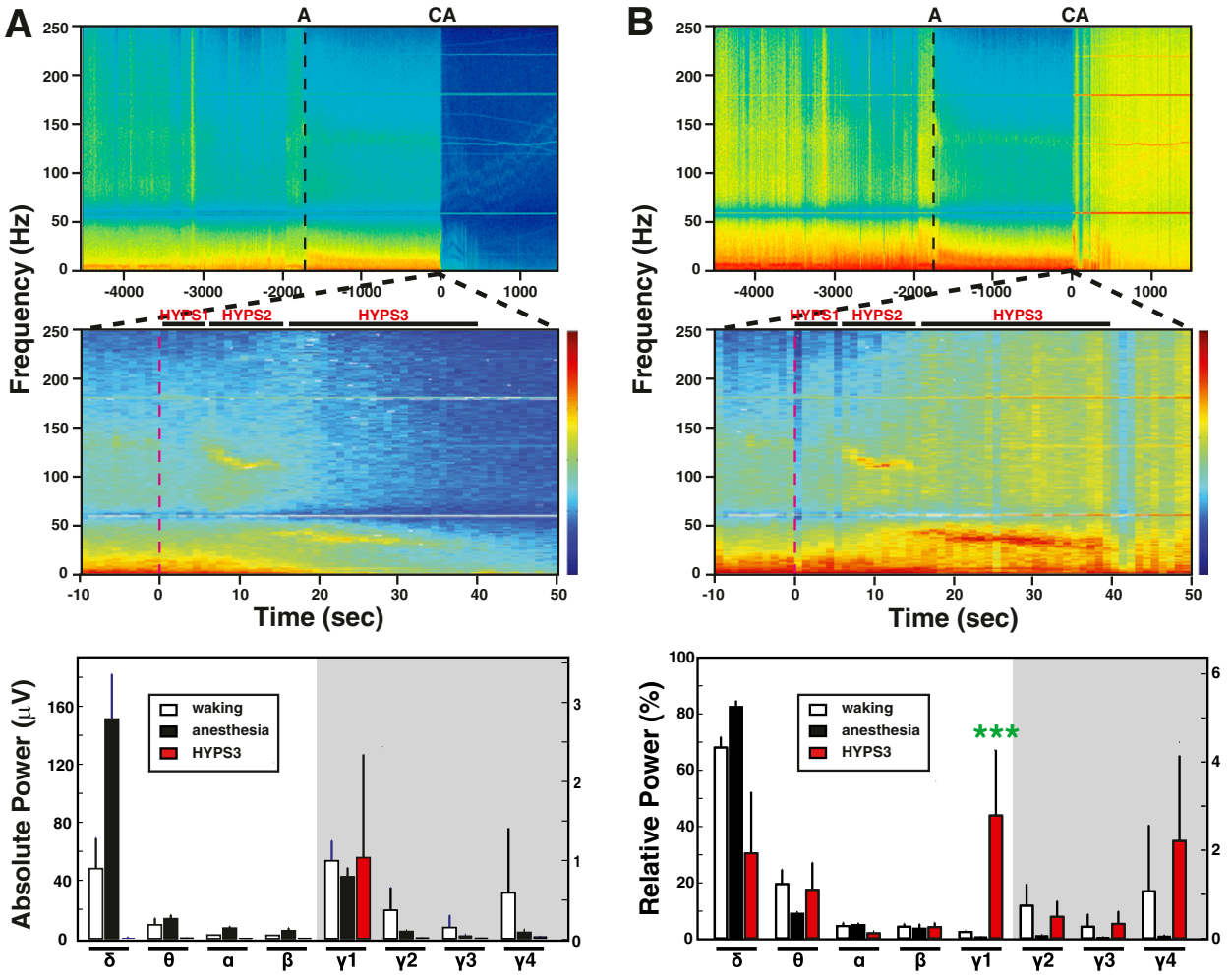

Fig. S3. Gamma power increases following CO_2 inhalation. (*A*) The spectrograms of absolute power averaged over the six EEG channels during waking, anesthesia, and following cardiac arrest. A representative rat (ID5520) is shown (*Top* and *Middle*), and averaged values for eight rats are shown at *Bottom*. Time is relative to the moment of CO_2 inhalation (CO_2; T = 0 s), and the time of ketamine/xylazine administration was marked as A on top of the graph. (*Middle*) EEG power around the time of CO_2 administration is displayed in an expanded scale, which shows 10 s of anesthetized state and 50 s of hypoxia. The time of CO_2 inhalation, defined as T = 0 s, is marked as a red dashed line. The *z* axis of spectrograms (*Middle*) uses a log scale, with blue indicating low power and red denoting high power. Three distinct stages of EEG power were detected following respiratory arrest: hypoxia state 1 (HYPS1), HYPS2, and HYPS3. The absolute power of eight frequency bands from eight rats was compared during waking, anesthesia, and HYPS3 states (*Bottom*). During waking and anesthesia, the mean and SD of power were calculated with 10-min EEG epochs, and taken from the middle of both (waking and anesthesia) 30-min periods. HYPS3 values were derived from the peak powers (2-s bin). Whereas slower bands (delta, alpha, and beta) exhibited significant ($P < 0.001$) decline in power, gamma bands, especially low-gamma bands, showed comparable power density at near-death compared with waking state ($P = 0.9962$ between waking and HYPS3, $P = 0.8625$ between anesthesia and HYPS3). (*B*) All gamma bands showed significant ($P < 0.05$) increases in relative power following hypoxia compared with the anesthetized state, whereas theta band at near-death showed a significant increase to a level indistinguishable with the waking state (*Bottom*; $P = 0.7913$ between waking and HTPS3). Of the analyzed frequency bands, the low-gamma bands showed the most striking increase in relative power at near-death compared with both the waking state and the anesthetized state ($P < 0.005$). (*Bottom*) Vertical axis on the right side applies only to the gamma bands within the gray shaded areas.

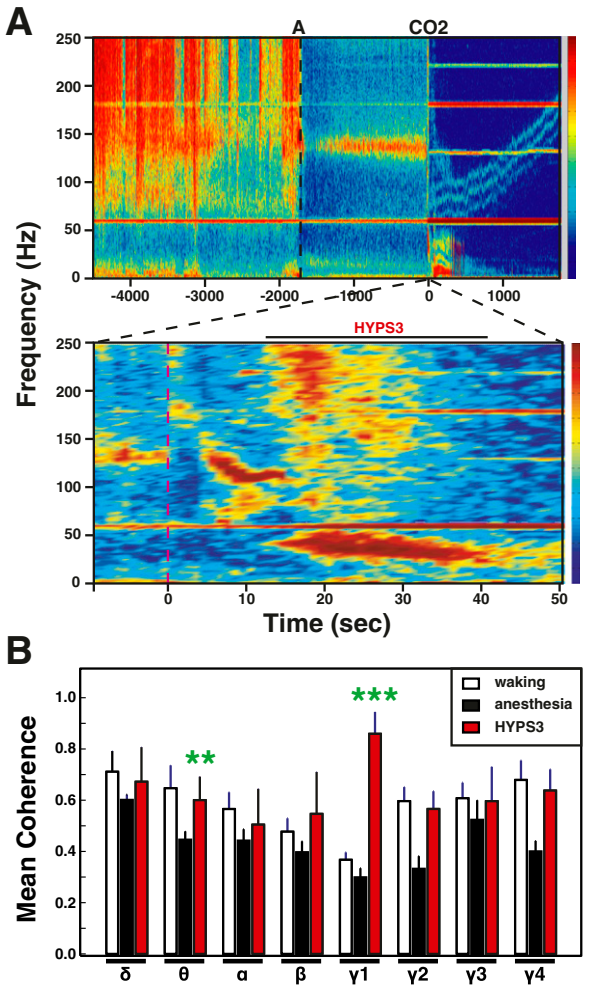

Fig. S4. Gamma coherence is markedly elevated after global hypoxia. (*A*) Mean coherence values over six EEG channels during waking, anesthesia, and following CO_2 inhalation are shown for one representative rat (ID5520). A narrow window of sharply increased coherence occurs across all frequency bands and is clearly detectable immediately following hypoxia (*Upper*); an expanded analysis is shown in *Lower*. Elevated coherence is evident for low-gamma (25–55 Hz) bands (13–42 s). The *z* axis indicates the degree of coherence, with blue indicating low levels and red indicating high levels of coherence. (*B*) The mean and SD of EEG coherence from six different locations were computed for eight indicated frequency bands during three states ($n = 8$). Low-gamma ($\gamma 1$) oscillations displayed a significant ($P < 0.0001$) increase in coherence compared with the waking and anesthetized states. Theta coherence showed a significant ($P < 0.01$) increase during HYPS3 compared with the anesthetized state and is indistinguishable from the waking state ($P = 0.4809$ between HYPS3 and waking). Error bar denotes SD (**$P < 0.01$, ***$P < 0.001$).